MIMO Antenna Array in 5G Communication

Wentao Song

College of Information Engineering, Shanghai Maritime University, Shanghai, 200135, China.

202010320034@stu. shmtu. edu. cn

Abstract: The main topics of this study are the fundamental operation of a MIMO antenna array and the benefits of using MIMO technology for 5G communication. Three significant works are recognized as benchmarks by outlining the component sets and spatial reuse that designers should consider in MIMO antenna design. For 5G low and medium frequencies, these include an 8x8 large-scale MIMO antenna array and a circular binary MIMO antenna array. In these designs, the design of the MIMO antenna array will be carried out based on the introduction of the design and parameter selection of the antenna array elements as a priority. Additionally, this study conducts a performance analysis of a multi-cell, Massive MIMO antenna array system, which serves as a high reference point for the Analysis of this system. Numerous possible application domains exist for the study object of this work, including hotspot situations and 3D coverage scenarios. Campus, shopping malls, and halls are examples of hotspot environments.

Keywords: MIMO, Antenna Array, 5G Communication.

1. Introduction

Since the 1980s, mobile communication technology has experienced 5 generations of mobile communication systems. The first generation of the mobile communication system (1G) is based on analog technology Frequency Division Multiple Access (FDMA). The second generation of the digital cellular communication system (2G) is based on Time Division Multiple Access (TDMA) and FDMA. The third generation of the communication system (3G) is mainly characterized by Code Division Multiple Access (CDMA). And the fourth generation of the communication system (4G) is primarily characterized by orthogonal frequency division multiplexing technology (OFDM) and MIMO. The key components of fourth-generation communication systems are OFDM and MIMO [1]. Single-input single-output (SISO) systems have a limited ability to transmit information during the transmission and reception of signals in the prior iteration of wireless communication. As a result, MIMO becomes a crucial technology for mobile communication systems of the fourth generation [2].And in today's 5G society, 5G needs higher performance than 4G. It needs to reach peak rates of 10-20Gbit/s, have spectrum efficiency to improve more than 3 times than LTE (Long Term Evolution), and to have the ability to connect devices within a large area to accommodate IoT communications. Therefore, Massive MIMO technology is particularly important, it can achieve effective use of the multipath effect, the traditional antenna in the vector channel into a matrix channel, to achieve spatial gain and multiplexing, and to achieve the goal of spatial diversity gain, beam focussing effect to achieve full sharing, is one of the important technologies to solve the problem of exponential growth of wireless data services growth. [3,4] But so far, the communication array antenna arrangement proposed to meet the construction of 5G base stations is still a high-cost project, so the design solution of antenna array is the key to reduce the construction cost and improve the efficiency.

In recent years, MIMO antenna technology has advanced, and in 2016, China Datang Mobile held the "5G integrated verification platform and 256 Massive antenna" conference, the first to demonstrate the world's leading Massive MIMO super Massive antenna technology, PDMA new multi-access technology and Telematics technology. [5]

Over the years, MIMO technology has undergone a qualitative leap from single-user to multi-user and then to massive MIMO technology. The original single-user MIMO technology is only point-to-point propagation, but there are inter-user interference problems to meet user needs. Later multi-user MIMO technology to solve the problem of inter-user interference between users, but there is a new

problem of inter-cell interference. Therefore, Massive MIMO technology has now emerged to improve the utilization of space resources and spectrum efficiency fully. [6] And at the time of 4G society, the number of antennas per group did not exceed four, but nowadays, $16/32/64/128$ or even larger antennas are supported in the massive MIMO technology. [7,8]

After the introduction of Massive MIMO technology in 5G, its wireless product form has become more abundant. These products have different coverage capabilities. Although it is more difficult to effectively match Massive MIMO technology with coverage scenarios due to the different parameter performance of various products, Huawei, ZTE, and other companies have proposed various adjustment schemes. [9]

This article explains the basic operation of a MIMO antenna array and the benefits of MIMO technology when used to 5G communication. In Chapter 2, designers should pay attention to component set and spatial multiplexing in MIMO antenna design, and three key works will be illustrated in Chapter 3. The authors will present the efforts of two designers in Chapter 3, which are 8 8 enormous MIMO antenna arrays and circular binary MIMO antenna arrays for 5G low and medium bands. The design and parameter selection of the antenna array elements will be introduced as a priority in these designs, and the design of the MIMO antenna array will be based on them. The performance study of a multi-cell, Massive MIMO antenna array system by a different author, who has a high reference value for the analysis procedure of the system, will also be included in this work. The study topic of this work includes a wide range of possible applications, including hotspot scenarios and 3D coverage scenes. Examples of hotspot settings include busy places like campuses, shopping malls, and music venues. Massive MIMO technology can offer great spatial multiplexing gain and powerful beamforming capabilities to address large capacity needs. High-rise buildings are one example of a 3D coverage scenario where beamforming in the context of Massive MIMO may significantly enhance horizontal and vertical coverage [8,10].

2. Principle of MIMO antenna

2.1 Application principle of MIMO technology

Massive MIMO networks use the spatial Degrees of Freedom (DoF) provided by antennas to transmit the same signal at each point where different phase-shifted antennas are applied. Thereby multiplexing information for users over the same time-frequency resources and focusing the radiated signal to the destination user, minimizing intra- and inter-cell interference. [10]

In practice, MIMO technology enables multiple line inputs/outputs for communication power, and also increases mobile communication capacity without adding additional resources to the broadband. In order to meet the increasingly newer network communication needs, research scholars continue to develop MIMO technology, i. e. , how to achieve higher efficiency or more reliable transmission behavior of communication in a given transmission line. [11]

When applying MIMO technology to 5G mobile communications, it can be divided into two main applications: diversity and spatial multiplexing. Diversity mainly refers to the use of multiple wired transmission antennas to achieve the transmission and reception of signals. In practice, a diversity transmission method can effectively improve the reliability of the transmission process by reducing the possibility of transmission channel instability. Spatial multiplexing is mainly the use of multiple independent antennas in space to achieve the transmission of network signals. The application of this technology can effectively widen the information transmission path and provide effective support for improving data transmission efficiency. [2]

In 1948, Claude Elwood Shannon proposed Shannon's theorem $Blog_2(1+s/n)$ in "Mathematical Principles of Communication". According to Shannon's theorem, a communication system's operational bandwidth, antenna transmit power, and noise power may all be increased to increase the channel capacity [9,12]. Among them, multi-antenna approaches can dramatically expand the system channel capacity by fully using dimensional spatial resources. The expression for the channel capacity in the multi-antenna scenario is $C = \min(m,n)Blog_2(1+s/n)$, where min(m,

n) is the maximum value of the channel model rank, and the minimum value among the number of transmitting antennas m and the number of receiving antennas n is taken.

In 2010, Marzetta proposed the theory of Massive MIMO (MIMO). The number of Massive MIMO antennas was expanded to 64. The vertical beam was added. Combined with beam fugacity has the advantages of strong coverage performance, high spectral efficiency, large network capacity, and low cell interference [9,13]. With Massive MIMO technology, the antennas have different horizontal flap angles, vertical flap angles, direction angles and down tilt angles in different Pattern configurations. Then different patterns of beams will be obtained, so that different kinds of scenes, such as roads, tall buildings and squares, can be covered with different broadcast beams to achieve the best coverage effect.

2.2 Massive MIMO antenna array in patch form with gap-coupled feed

In conventional communication systems, antenna arrays usually use eight-cell one-dimensional line arrays, but such arrays cannot perform two-dimensional beam scanning. In addition, the cross-crossed symmetrical oscillator form of antenna array cells used in this antenna array needs to balance the Barron feed, and the processing cost is high, difficult and takes up a lot of space. And another new antenna array with 64 RF channels and 256 cells of single-polarized microstrip antenna array applied to 5G communication system is proposed later. Although the cells occupy small space and have simple structure, it cannot realize bipolar specialization at 5.8GHz operating frequency [14]. The first new 8×8 large-scale MIMO antenna array for fifth-generation mobile communication systems is proposed below. The antenna elements of this array are in the form of gap-coupled feed patches, which are fed separately through two ports. This MIMO antenna array can achieve ±45° dual polarization characteristics in the operating band, which improves some problems of the new design mentioned above. In addition, this design has the advantages of low profile and compact structure compared to the traditional cross-crossed oscillator design form, which does not require balun and is easy to integrate with the RF front-end design [1].

2.3 MIMO circular antenna design based on 5G low-frequency band

MIMO technology can increase the signal transmission speed, improve spectrum utilization, and increase the stability and reliability of communication without increasing the transmit power and requiring additional spectrum [15,16]. This satisfies the data rate requirements of 5G, so designing MIMO antenna arrays in the main 5G frequency bands is essential for 5G development. The design idea of the second MIMO antenna array proposed in this paper focuses on two main points: making full use of the diversity technique and increasing the isolation.

Diversity technology can break the physical limit of Shannon capacity without increasing the transmit power, greatly improving the rate and reliability of channel transmission, not only that, diversity technology can also improve the isolation of the port [17].

The ports need sufficient isolation if the MIMO system obtains good diversity gain. In general, the spacing between antenna array elements should be greater than or equal to the half-wavelength corresponding to the antenna's operating frequency [17]. However, today's smart and mobile portable devices require the antenna size to be as small as possible. The spacing between the antenna elements cannot be too large. Therefore, we can improve this problem by adding an isolation network and ground slotting.

Isolation networks improve the isolation by blocking the current between ports at a specific frequency. A network structure for improving isolation has been proposed in the literature [18]. This structure cuts off the current between the two antenna elements and improves the isolation by 6-16 dB in the antenna operating band.

Slotting on the ground plane is also a common method to increase isolation. The literature [19] proposes a dual “T” shaped MIMO antenna with dual frequency bands. The slotted ground plane makes the port isolation of the dual-port MIMO antenna reach below -15dB, which meets the engineering requirements.

2.4 Performance Analysis of Multi-Cell Massive MIMO Systems

Massive MIMO systems often reduce interference between users by arranging large antenna arrays at the base station, eliminating uncorrelated noise, and enabling more accurate beam assignment, substantially increasing spatial freedom and improving signal quality. At the same time, the system performance can be improved by reducing the amount of user transmit power at the base station while keeping the system capacity unchanged. In the case of multi-cell, large-scale MIMO systems, multi-cell interference and pilot frequency pollution in the system, which affects the system rate [20]. So the performance of the multi-cell, large-scale MU-MIMO system in the literature [21] will be studied next.

3. Analysis of the realization path and results of the design body

3.1 8 × 8 massive MIMO antenna array

The design is derived from the literature [1]. The structure of the antenna array element, from top to bottom, is the metal radiating patch, the air layer, the upper floor layer etched with H-shaped slits, the upper dielectric substrate layer, the feed strip line layer, the lower dielectric substrate layer, and the lower ground plane layer. The dielectric substrate is the commonly used Rogers RT/duroid 5880 with a thickness of 1 mm and a relative dielectric constant of 2. 2.

The two H-shaped slits on the upper floor are designed to reduce coupling between the ports [22]. After the excitation signal is introduced by the feeder strip line, it will be coupled by these two H-shaped slits and thus excite the metal radiation patch. Figure 1 shows the effect of the H-shape dimension on the reflection coefficient. After consideration, the designer used to set the length of the long slit in the middle to 30 mm and the length of the short slit on both sides to 6 mm.

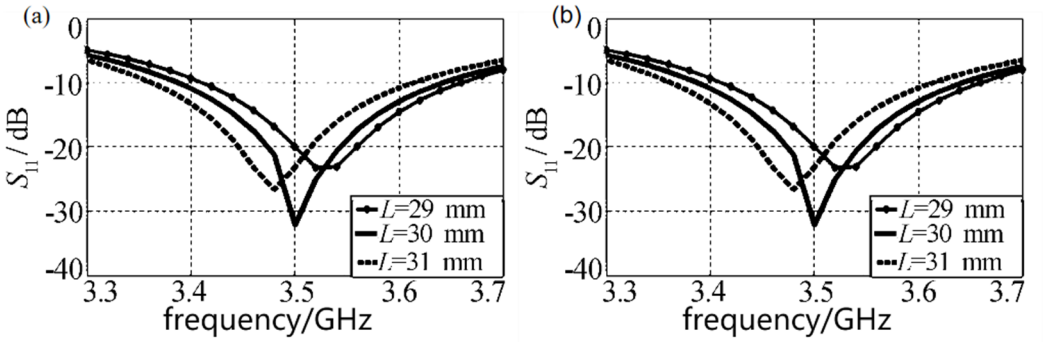


Figure 1. (a)The variation of reflection coefficient with L.(b)The variation of reflection with l [1]

This caliber-coupled electromagnetic coupling type feed structure can effectively suppress the additional radiation from the feeder strip line. And in order to eliminate the bi-directional radiation problem caused by the conventional slit-coupled feed, the feed line here is in the form of a ribbon line.

The signal is introduced through two ribbon line feed ports and coupled through two H-shaped slits on the upper floor to excite the metal patch. The metal patch, the feed line and the coupling gap are rotated by 45° with respect to the dielectric substrate to achieve ± 45° dual polarization radiation. In this structure, metalized isolation vias are incorporated between the slits to reduce coupling between the ports. In addition, metallized through-holes are also incorporated on both sides of the ribbon line, which effectively suppresses the high secondary modes generated during the transmission of the ribbon line [23].

The designer requires the reflection coefficient of both ports to be less than -10. Based on the equation $W_{patch} = \frac{c}{2f\sqrt{\varepsilon_r}}$and the graph in Figure 2 about the variation of reflection coefficient with edge length, the designer uses 32 mm as the patch edge length.

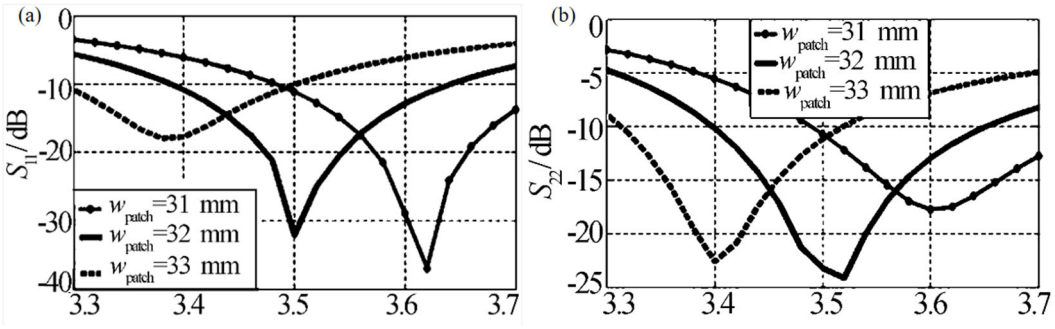


Figure 2. (a) The variation curve of reflection coefficient with the edge length of the one-port patch.(b) The variation curve of reflection coefficient with the edge length of the two-port patch.[1]

In addition, the thickness of the air layer in the cell structure affects the standing wave by influencing the amount of electromagnetic coupling between the gap and the patch. According to the effect curve of air layer height on standing wave in Figure 3, the designer decided to make the air layer height $2.5\ mm$.

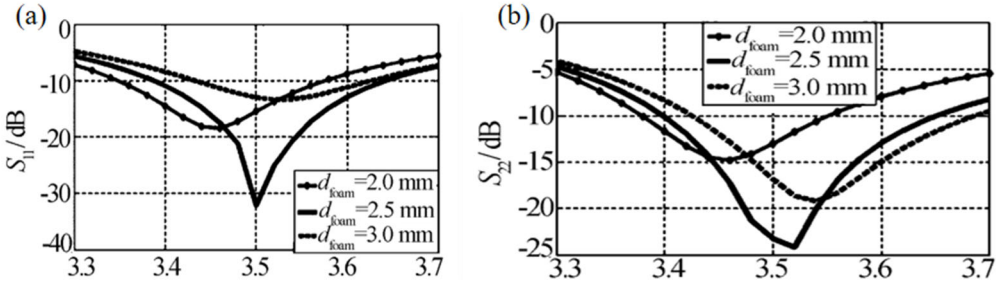


Figure 3. (a)Variation curve of standing wave with air layer height of one-port patch. (b)Variation curve of standing wave with air layer height of two-port patch [1].

Finally, the simulation results of the antenna array element are given.

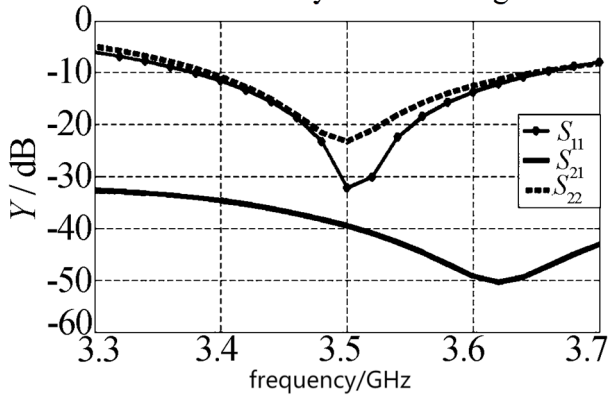


Figure 4. Antenna element simulation results [1]

This antenna array is small in size and is arranged in an 8×8 matrix. In order to suppress the grating, the array element spacing needs to satisfy the equation

$$\frac{d}{\lambda} \leq \frac{1}{1 + sin\theta_0} \tag{1}$$

Here the array element spacing choose $d_x = 48mm, d_y = 55mm$

The working band of the designer's array is chosen as 3.4GHz-3.6GHz, and 3.5GHz is chosen as the result case here in this paper.

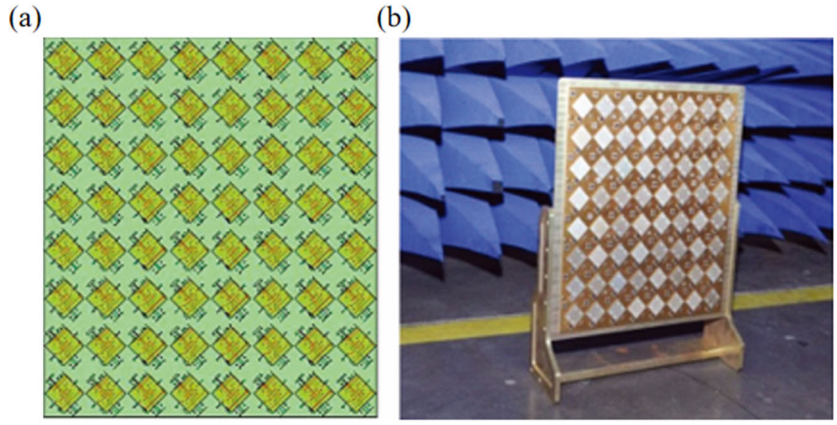


Figure 5. (a)Real-face simulation model.(b)Physical drawing [1].

From the simulation results of the E-plane and H-plane flaps with two polarization ports plus excitation at 3.5 GHz, it can be concluded that the beamwidth of the elements in the array is close to $\pm 56°$, and the cross-polarization ratio in the maximum radiation direction is greater than $20\ dB$. In the beam range of $\pm 56°$, the cross-polarization ratio is greater than $16\ dB$.

3.2 Binary MIMO circular antenna array design

This section presents a circular MIMO antenna covering the low and medium frequency bands of 5G, citing literature [17], which feeds a circular radiating element through a microstrip line. The operating mechanism of a single circular antenna is first analyzed, and then the port isolation is improved by grouping the array with two circular antennas and then introducing slotting and adding an additional isolation network on the ground plane. Finally, the designer's test results will be given.

Figure 6 shows the antenna element structure. In this design, the substrate material used is FR4 with $\varepsilon_r = 4.4$ and the substrate thickness is $1.6\ mm$. the size of the half-slotted ground plane on the back side of the substrate is $40mm \times 21.1mm$ and the size of the small rectangular slot added to match the impedance is $3.5\ mm \times 3\ mm$. the radiating element is circular with an inner diameter of $4.5\ mm$. and the overall size of the antenna element is $40mm \times 50mm \times 50mm$.

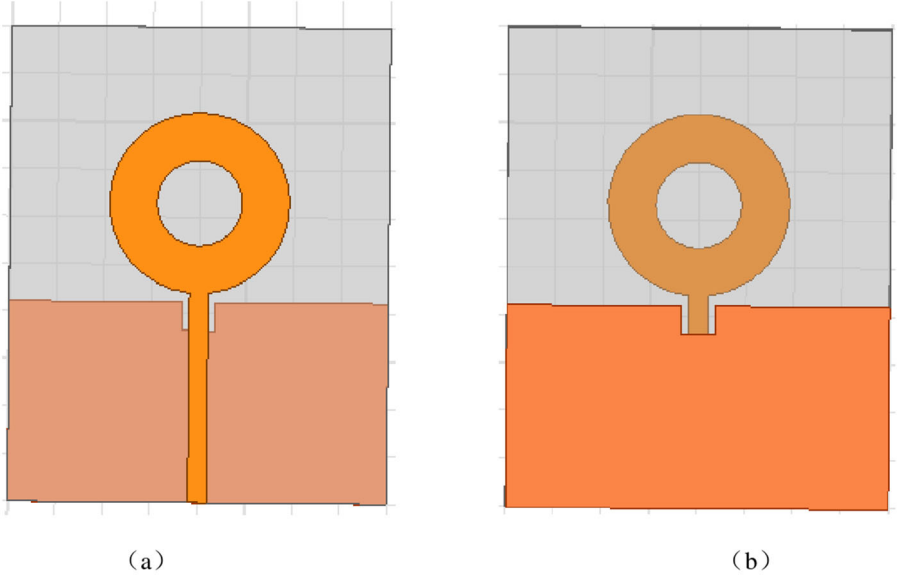


Figure 6. Antenna element structure diagram[17]

Because the outer diameter of the ring will affect the antenna performance, the outer diameter is not given above. Figure 7 is the curve designer gives, which is the effect of outside diameter on the reflection coefficient. Observing the curve can be derived from R2 (antenna outside diameter)

increases, the antenna work frequency point to a low-frequency direction, which means the larger the size, the lower the frequency, the larger the wavelength. This is in line with the size of the common transition effect. Through software simulation, the size of R2 is finally determined to be 9. 5mm. At this time, the working frequency band of the antenna includes 3300-3600MHz and 4800-5000MHz, and the reflection coefficient of the antenna is very small in the working frequency band.

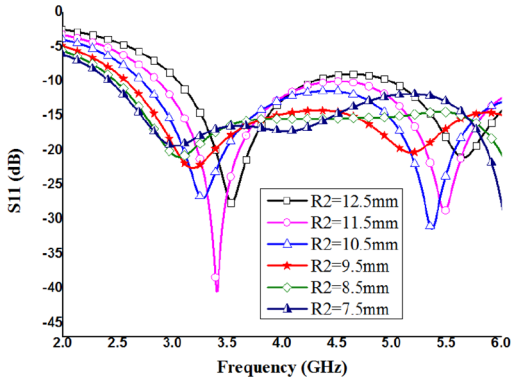


Figure 7. Effect of antenna's outer diameter on S1,1 [17]

In Figure 7, it is obvious that the antenna has resonance points around 3. 3GHz and 5200GHz. The multi-frequency radiation mechanism of the antenna is analyzed as follows: the radiation element is circular in shape. The current is fed from the outer end of the circular, arriving at different places, and passing through different paths, thus producing different frequency points [17]. From Figure 8, we can see that the low-frequency point of the surface current is concentrated in the lower part of the ring. The high-frequency point of the surface current is concentrated in the middle and upper part of the ring, so changing the ring's outer diameter will change the current path's length and the operating frequency point of the antenna.

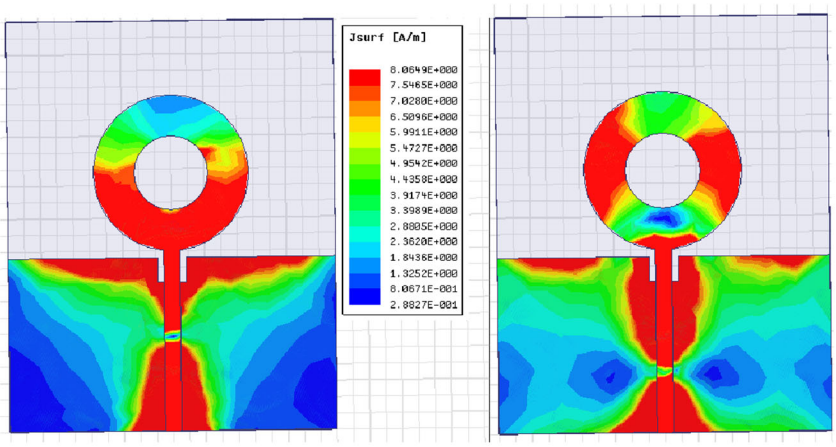


Figure 8. Antenna element surface current distribution [17]

Based on the above antenna element, a binary antenna array is given. The material and thickness of the substrate remain the same and the overall size of the antenna is changed to $70mm \times 50mm \times 1.6mm$. Two circular radiating elements, as described above, are placed on the front side of the substrate. Since this is a binary antenna array, the rectangular slot alone cannot meet the engineering requirements, so the designer has improved the rectangular slot made to improve the isolation. The slotted ground plane designed by the designer on the back side of the substrate consists of a large rectangular slot, two small L-shaped slots and a raised link. Figure 9 shows the structure of this MIMO binary antenna array.

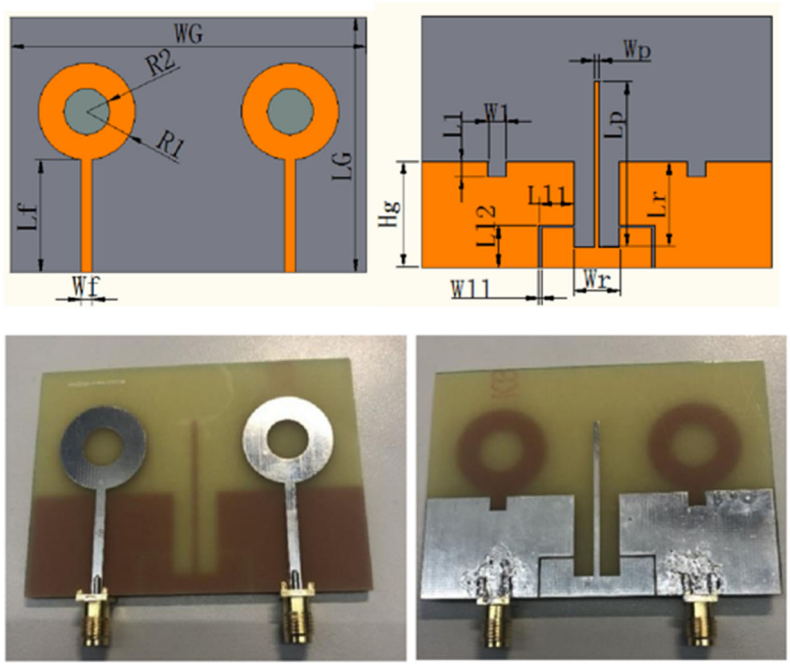


Figure 9. The schematic and physical diagram of MIMO antenna structure.[17]

The change in the ground plane would cause the coupling between the ports to decrease and the isolation to improve, so the change of S2,1 parameter was simulated by HFSS software. Finally, the improved S2,1 parameter was below -20dB, which satisfied the engineering requirements. Figure 9 shows the physical diagram of the antenna made by the designer.

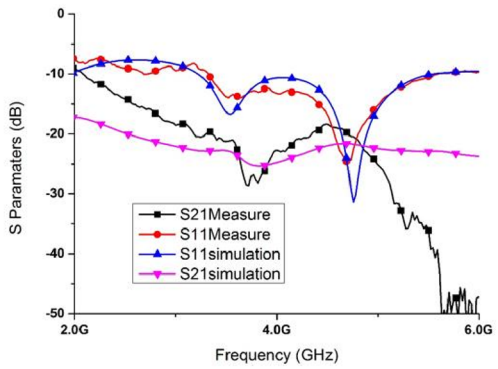


Figure 10. S-parameter curves for antenna simulation and testing [17]

From Figure 10, we can see that there are deviations between the actual measured values of S-parameters and the software simulated values, such as polarization point shifts and reflection coefficient amplitude variations. This phenomenon may be caused by processing errors and material instability. This error may be caused by the loss caused by the equipment during the actual test.

According to the working frequency band of the antenna, the designer selected the center frequency point of the two bands, the antenna far-field directional map test at 3. 5GHz and 4. 9GHz, the test results are shown in Figure 11. Figure 11.(a) is the antenna port one excitation, port two connected to match the load. The antenna in the 3.5GHz frequency point test to get the E surface and H surface radiation direction map. Figure 11. (b) is the antenna port one excitation, port two connected to match the load, the antenna in the 4. 9GHz frequency point test radiation direction of the E surface and H surface diagram.

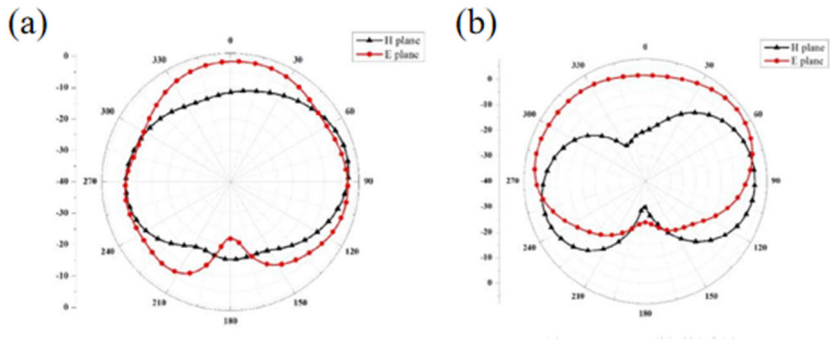


Figure 11. (a)Radiation pattern at 3.5GHz.(b)Radiation pattern at 4.9GHz.[17]

Figure 12 gives the curve of the maximum gain of the antenna with frequency in the antenna working frequency band. The maximum gain of the antenna at 3. 5GHz is 1. 5dBi, and at 4. 9GHz, the maximum gain of the antenna is 3dBi.

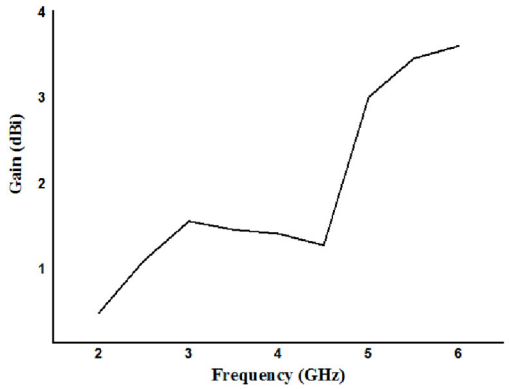


Figure 12 Antenna gain curve[17]

Therefore, the binary MIMO antenna covers 3300-3600MHz and 4800-5000MHz in the low and medium frequency bands of 5G, with good radiation characteristics and isolation.

3.3 Performance Analysis of Multi-Cell Massive MIMO System

For a Massive MIMO system with multiple cells, the system consists of L cells in a hexagonal shape with a base station at the center of each cell with M antennas. It is assumed that there are K single-antenna users in each cell, satisfying the massive MIMO system condition, i. e. , $M \gg K$. In addition, it is assumed that each cell uses the same frequency resources, i. e. , the frequency reuse factor is 1, and the whole system operates in TDD mode [21].

Figure 13 illustrates a Massive MIMO system with three cells. Each base station performs ZF filtering on the received signal at the same time-frequency resource in the uplink reception. The base station in each cell receives useful signals from users and interfering signals from all users in other cells to the base station.

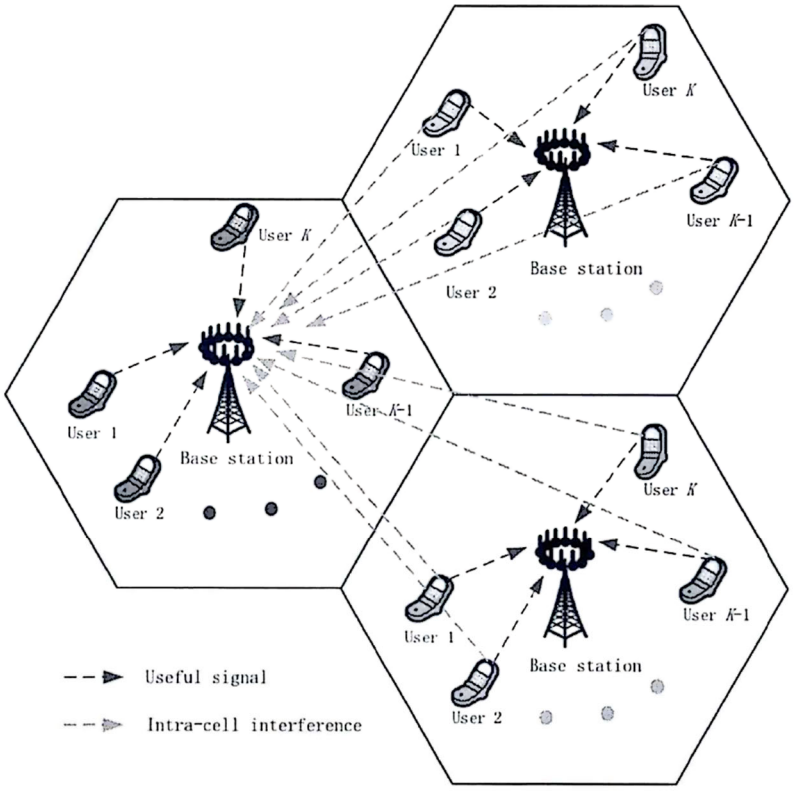


Figure 13. Model of multi-cell massive MIMO system [21]

In addition, each base station using ZF reception still needs to know the CSI of the user, which requires uplink training for estimation. That is, at the beginning of each channel coherence interval (T), each user transmits a lead sequence of length τ to the base station where it is located, which obviously satisfies $T > \tau$. Theoretically, the lead sequences of all users in all cells should be orthogonal so that there is no lead contamination during the uplink training. However, to do so requires that the length of the guide frequencies satisfies at least $\tau \geq LK$, which will reduce the subsequent data transmission time since the channel coherence interval is fixed. For this purpose, the users in the cell use an orthogonal set of guide frequency sequences, and this orthogonal set of guide frequency sequences is reused in all cells. This guarantees the data transmission time but also introduces guide frequency pollution during the channel estimation phase, reducing the CSI's estimation accuracy. [21]

The designer obtains a non-perfect CSI, uses the estimated channel matrix to obtain the uplink rate and rate bounds, and concludes that the upper bound has very tight characteristics. This paper focuses on the simulation results of this design, so the above conclusion acquisition process is not developed in detail.

Figure 14 shows the uplink rate of the first cell and its upper bound. The figure shows that the upper bound is close to the simulated reachable rate, which confirms that the upper bound is very tight. It can be analytically concluded that increasing the length of the lead sequence τ from K to 4K improves the system rate in the low SNR regime. However, increasing the lead length in the high SNR regime worsens the system rate. This upper bound result also applies to the single user rate within a single cell [21]. The designer also derived that the difference between the upper and lower bounds decreases monotonically with the increase in the number of antennas at the base station. This is shown in Figure 14. (b).

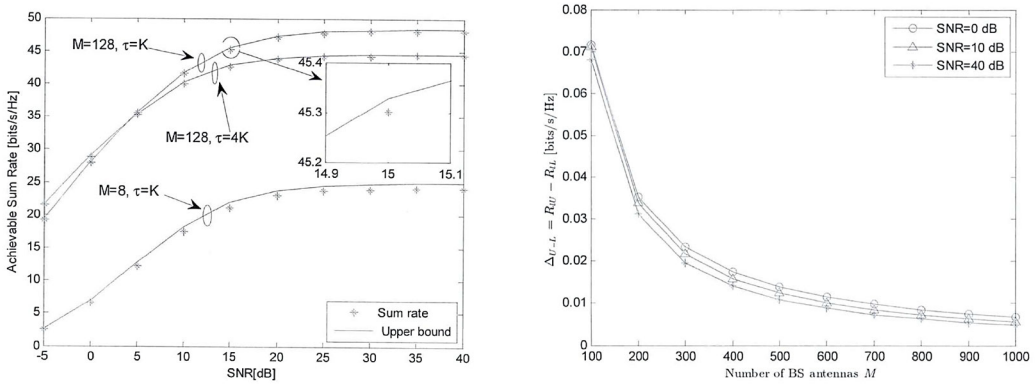


Figure 14. (a) Uplink rate and its upper bound (b)Difference between upper and lower bounds vs. number of antennas at the base station [21]

Overall, the authors of this literature theoretically prove that the upper bound on the rate of Massive MIMO systems is tight. This result provides a theoretical basis for multi-cell, Massive MIMO systems.

3. 4 contrast

Comparison	Advantage	Disadvantage	Performance	Application scenarios
8 × 8 massive MIMO antenna array	Low profile, compact and easy to integrate design	Limited to low frequency band	VSWR less than 2, S21 less than -23db in operating frequency	Mobile Devices
Binary MIMO circular antenna array	Small size and dual-band antenna	Limited to low frequency band	Good radiation characteristics and isolation degree in the operating frequency range	Improved system performance and partial elimination of interference
Multi-cell massive mimo system	High spatial freedom, accurate beam assignment, and high system performance	Interference between some users, high cost	Handheld mobile terminal	High-traffic areas

4. Conlusions

This paper mainly introduces the application of MIMO antenna technology in 5G communication and explains the application principle of MIMO technology in detail. It is emphasized that when designing the MIMO antenna array, it is necessary to focus on the actual engineering requirements and understand the implementation process of the two application methods of component integration and spatial multiplexing. After first designing the antenna element, it is important to focus on impedance matching, isolation, antenna polarization and other issues to be fully considered when the designer designs the antenna array based on this process. At the same time, when designing a multi-cell massive MIMO antenna array, when considering the antenna size, signal-to-noise ratio, and other issues, also consider the user's needs.

In order to better meet the 5G mobile communication channel capacity, the development of MIMO technology is the key to effectively widening the information transmission path and data efficiency. The development of this technology can also improve 4G networks. The relationship between channel capacity and parameters such as transceiver distance in tunnels will provide the basis for future tunnel subway traffic.

References

[1] Mao JJ, Yu DQ, and Jiao YC. “A large-scale MIMO antenna array design for 5G. ” Modern Radar 38. 2 (2016): 4.

[2] Sun, Xinjing, and Wang, Fang. “Analysis of MIMO technique in 5G mobile communication array antenna modeling. ” Changjiang Information and Communication 035-004(2022).

[3] Wu, G. K.. “Analysis of large-scale MIMO antenna arrays for 5G. ” Information and Computers 16(2018):2.

[4] Luan, Shuai et al. “Analysis of large-scale MIMO antenna design and its impact on 5G systems. ” Post & Telecom Design Technology 7(2016):5.

[5] Huang, Haifeng. “Datang Cai Yuemin: Massive MIMO will be the earliest to realize 5G technology for 4G. ” Communication World 13 (2017): 1.

[6] Wang, Dianhai [1]. “An analysis of developing large-scale MIMO technology in 5G communication. ” Science and Information Technology 18(2018):2.

[7] Cui, Juanjuan et al. “A review of millimeter wave MIMO antenna technology research in 5G wireless communication systems. ” Electronic World (2019).

[8] Wei, Chao. “Research on Massive MIMO technology in 5G mobile communication. ” Science and Technology Wind 16(2020):1.

[9] Zhang, Yejiang et al. “Study on the application of Massive MIMO technology in 5G network optimization. ” Digital Communication World.

[10] Li, X. Y. et al. “Study on the application of large-scale MIMO technology in 5G. ” Digital Communications World 10(2019):2.

[11] Lin, L. , and Wei, K.. “MIMO technique in 5G mobile communication array antenna modeling study. ” Communication Power Technology (2021).

[12] Zhao, Yunfeng et al. “Research and practice of 5G multi-antenna technology. ” Jiangsu Communication 36. 5(2020):6.

[13] Guang-Ling Zou, and Cai-Hua Pan. “Exploration of 5G scenario-based network regulation scheme. ” ZTE Technologies 26. 2(2020):5.

[14] Pang, et al. “Design and Implementation of an Active Multibeam Antenna System with 64 RF Channels and 256 Antenna Elements for Massive MIMO Application in 5G Wireless Communications. ” China communications: China Communications 11. 11(2014):16-23.

[15] GoldsmithA. , et al. “Capacity limits of MIMO channels. ” IEEE Journal on Selected Areas in Communications (2006).

[16] Cui, Shuguang , A. J. Goldsmith , and A. Bahai. “Energy-efficiency of MIMO and cooperative MIMO techniques in sensor networks. ” IEEE Journal on Selected Areas in Communications 22. 6(2004):p. 1089-1098.

[17] Yizhong Wu. Research on millimeter wave microstrip MIMO antenna for fifth generation mobile communication. Diss. University of Electronic Science and Technology.

[18] Alsath, M. G. N , M. Kanagasabai , and B. Balasubramanian. “Implementation of Slotted Meander-Line Resonators for Isolation Enhancement in Microstrip Patch Antenna Arrays. ” IEEE Antennas & Wireless Propagation Letters 12. 1(2013):15-18.

[19] Zhao, W. , et al. “Dual-band MIMO antenna using double-T structure for WLAN applications. ” 2014 International Workshop on Antenna Technology: “Small Antennas, Novel EM Structures and Materials, and Applications” (iWAT) IEEE, 2014.

[20] Hoydis, J. , S. T. Brink , and M. Debbah. “Massive MIMO in the UL/DL of Cellular Networks: How Many Antennas Do We Need?. ” IEEE 2(2013).

[21] Wang Xinshui. Research on key technologies and performance analysis of large-scale MIMO for 5G. Diss. Beijing University of Posts and Telecommunications, 2018.

[22] Hienonen, S. , A. Lehto , and A. V. Raisanen. “Simple broadband dual-polarized aperture-coupled microstrip antenna. ” Antennas and Propagation Society International Symposium, 1999. IEEE IEEE, 1999.

[23] POZAR D M. Microwave engineering [M]. New York: John Wiley&Sons, 2009